

Influence of interparticle electronic coupling on the temperature and size dependent optical properties of lead sulfide quantum dot thin films

Paul J. Roland, Khagendra P. Bhandari, and Randy J. Ellingson^{a)}

Wright Center for Photovoltaic Innovation and Commercialization, Department of Physics and Astronomy, The University of Toledo, 2801 W. Bancroft Street, Toledo, Ohio 43606, USA

(Received 19 November 2015; accepted 18 February 2016; published online 4 March 2016)

We report on the quantum dot (QD) size, temperature, and inter-dot coupling dependence on the optical absorption and emission for PbS QD thin films. Inter-dot coupling is induced by ligand exchange from oleic acid to 1,2-ethanedithiol, and the expected band gap red-shift observed for coupled QD thin films is accompanied by a modification to the temperature-dependence of the band gap energy. The amplitude and temperature dependence of the photoluminescence (PL) Stokes shift support recombination via a mid-gap state and also indicate that the application of band gap-specific models to fit the temperature dependence PL peak energy is inadequate. Electronically coupled QD thin films show PL quenching with decreasing temperature, following a Boltzmann model which is consistent with thermally activated carrier transport. Enhancing the inter-dot coupling results in the dynamic PL decay signal changing from single- to bi-exponential behavior, reveals a size-dependent transport activation energy, and yields a negative temperature dependent band gap energy for the smallest QD diameters. © 2016 AIP Publishing LLC.

[<http://dx.doi.org/10.1063/1.4943066>]

I. INTRODUCTION

Recently, lead chalcogenide quantum dot (QD) solar cells have achieved power conversion efficiencies as high as 10.7%¹ under standard photovoltaic test conditions. These colloidal QD-based devices are solution processable at room temperature, offering potential cost advantages in manufacturing over silicon and III-V material devices. The materials science and technological challenges of QD-based thin film solar cells are quite interesting from a fundamental standpoint, because thin QD film structure can exist anywhere within a range that spans from QDs which are fully isolated electronically—in which case transport is frustrated—to the case of fully merged QDs for which transport may be optimized but the benefits of quantum confinement are fully lost. The true colloidal QD solar cell therefore must balance confinement with electronic coupling to achieve efficient photocurrent collection while retaining the blue-shifted band gap energy to access the higher potential conversion efficiencies associated with the ~1.0–1.5 eV band gap range.

For weakly coupled inter-QD interactions, carrier transport within QD thin films has been found to occur via variable-range- or nearest-neighbor-hopping mechanisms. The transport activation energy is in this case dependent on inter-QD distance, QD diameter, semiconductor material, and dielectric function of the media between neighboring QDs. For example, Kang *et al.*² utilized an FET device architecture to probe the minimum energy for thermally activated carrier transport within PbSe QD thin films capped with 1,2-ethanedithiol (EDT, <10 meV for various diameters). In cases for which coupling strengthens via reduced inter-QD

spacing, increased volume-averaged dielectric constant within the film, and the resulting enhanced wavefunction overlap, band-like transport has been reported.³ Band-like transport correlates with scattering lengths that exceed the inter-QD distance, yielding improved mobilities that support high-performance QD photovoltaics.

To provide additional insights and understanding of transport properties within PbS QD thin films, we report here on investigations of the temperature dependent optical properties of films consisting of either coupled or isolated PbS QD thin films. There have been several studies of lead chalcogenide QD thin films reporting on the temperature dependent optical absorption,^{4–7} photoluminescence (PL),^{4,5,7–9} and time-resolved PL (TRPL);⁴ however, these studies either analyzed data from a subset of these optical methods or addressed only a single QD size. We report here on a complete set of data which, for the first time, utilizes multiple QD sizes to address the temperature dependence and inter-QD coupling dependence of absorption, PL, and TRPL. By investigating the absorption, PL, and TRPL, with respect to QD diameter, temperature, and QD thin-film interstitial capping ligand, we provide analysis of a single dataset for interpretation, free from variations in QD quality from different synthesis routines. The QD diameters investigated during this study were 2.7 nm, 3.1 nm, and 3.5 nm, with either oleic acid (OA) or EDT as the capping ligands. Based on the capping ligand size (OA ≈ 20 Å, EDT ≈ 6 Å), ligand exchange from OA to EDT substantially reduces inter-QD spacing and thereby enhances the inter-QD coupling to facilitate efficient carrier transport.¹⁰ As described below, the size-dependent PL quenching and large Stokes shifts support the model of a mid-gap state whose energy level is a function of quantum confinement.⁵ In addition, this work serves as a check on the previous reports of how the optical properties of coupled and

^{a)}Author to whom correspondence should be addressed. Electronic mail: randy.ellingson@utoledo.edu.

uncoupled PbS QD thin films vary with QD size and with temperature.

II. EXPERIMENTAL METHODS

A. Synthesis and thin film preparation

The PbS QD samples were synthesized using a slightly modified version of Hines and Scholes.^{11,12} After a non-solvent precipitation wash, the final product is re-suspended in anhydrous hexane. The size distributions for samples of average diameter 2.7, 3.1, and 3.5 nm were approximately $\pm 5\%$ based on the linewidth of the first exciton peak.¹³ Quantum dots capped with OA were cast into films via spin coating at 1000 rpm from a solution of approx. 100 mg/ml concentration; OA capped QD films contain nominally isolated QDs which exhibit no evidence of inter-QD coupling. Coupled QD films were created by the layer-by-layer technique (LbL, described elsewhere),¹⁰ utilizing 0.1 mM EDT in acetonitrile as the ligand exchange solution; solutions of OA-capped QDs with concentrations of approximately 6 mg/ml were utilized for the LbL depositions. All films were deposited on 1 mm thick borosilicate microscope slides cleaned via ultrasonic bath with Micro-90[®] cleaning solution and de-ionized water. For the three QD diameters investigated here, 2.7 nm, 3.1 nm, and 3.5 nm, films were deposited utilizing each capping ligand (OA and EDT). Replacing OA with EDT reduces edge-to-edge inter-QD spacing to ~ 0.25 nm^{14,15} which, due to increased wavefunction overlap of neighboring QDs, reduces quantum confinement as evident in a red-shift of the first exciton absorption.^{16,17}

B. Optical spectroscopic measurements

Samples were placed in a Janis VPF-100 pour-fill LN₂ cryostat, which was evacuated to a pressure of $\sim 7 \times 10^{-5}$ Torr for temperature-dependent optical transmission measurements; a closed cycle helium cryostat (Advanced Research Systems) was used for steady-state and time resolved PL measurements. Optical absorption measurements were conducted using a Perkin Elmer Lambda 1050 ultraviolet/visible/near infrared (UV/VIS/NIR) spectrophotometer. Steady-state PL spectra were acquired via lock-in detection using a frequency-doubled Nd:YAG laser as the 532 nm excitation source at 6.3 W/cm² and a liquid nitrogen cooled Germanium detector (Electro-Optical Systems), utilizing an optical chopper at 532 Hz and Horiba iHR320 monochromator [1200 g/mm; 750 nm blaze]. Time-resolved PL data were collected using a Fianium photonic crystal fiber laser source (SC400-2), an Acousto-Optical Tuning Filter (AOTF), a Horiba iHR320 monochromator [1200 g/mm; 750 nm blaze], a Hamamatsu NIR photomultiplier tube (PMT) (H10330A-25), and a Becker-Hickl SPC-130-EM Simple Tau system for time-correlated single photon counting. Depending upon the sample capping ligand, QD diameter, and temperature, the TRPL time window was selected for optimal data acquisition parameters. Quantum dot films were excited at a fluence of $\sim 2 \times 10^{12}$ photons·cm⁻²·pulse⁻¹ (632 nm) to attain sufficient detection events at higher temperatures; lower excitation levels were tested to confirm that the

high photon flux did not cause non-linear recombination dynamics arising from multi-exciton or Auger recombination. All of the raw data for absorption, PL, and TRPL data are included in spreadsheet format in the supplementary material.

III. RESULTS AND DISCUSSION

A. Optical absorption

As has been reported previously,⁴ the temperature dependent optical absorption measurements (Figure 1) show an overall increase in optical absorption with decreasing temperature. As shown in Figure 1, and quantified within Figure 2, the temperature dependence of the first exciton transition energy (dE_1/dT) extracted from a linear fit is found to decrease in value with decreasing QD diameter for both the case of OA- and EDT-capped QD thin films. While many semiconductor materials exhibit a *decreasing* band gap with increasing temperature, the band gap energy increases with

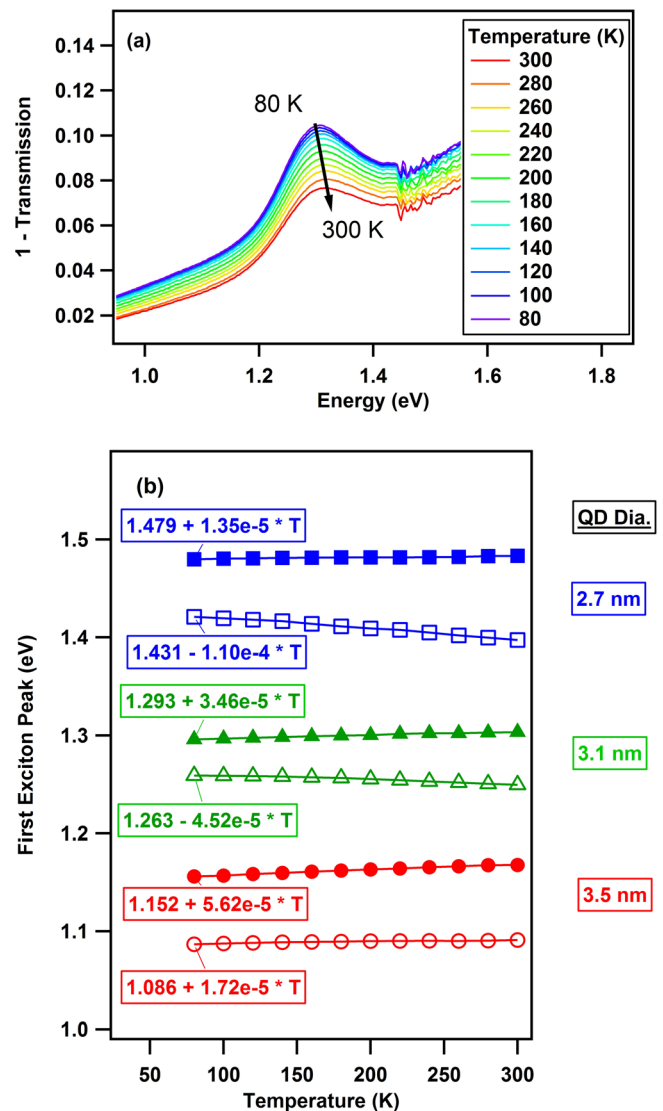


FIG. 1. (a) Temperature dependent optical response for the 3.1 nm OA capped PbS QD thin film, representative of the other films. (b) First exciton peak position (E_1) vs. temperature for the three PbS QD sizes capped with OA (solid markers) and EDT (hollow markers). Solid lines and equations are the results of linear fits of E_1 vs. T.

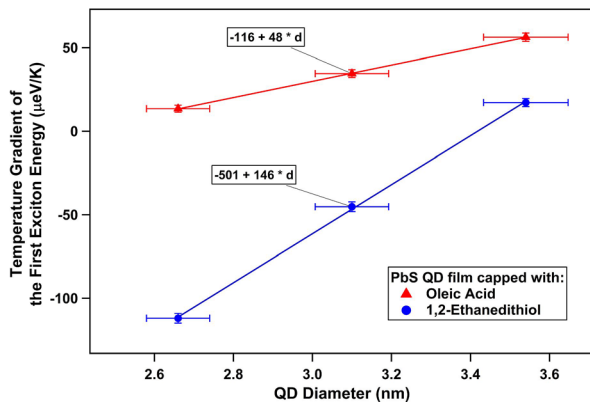


FIG. 2. Variation of the effective band gap temperature dependence, dE_1/dT , with QD diameter and capping ligand. For reference, the value of dE_g/dT for bulk PbS is $320 \mu\text{eV/K}$.

temperature for the bulk lead chalcogenides PbS, PbSe, and PbTe.¹⁸ For bulk semiconductor materials, the temperature dependence of the band gap energy arises principally from contributions of (a) thermal expansion (temperature dependence of the lattice constant, which modifies intrinsic bonding energies and atomic wavefunction overlap) and (b) electron-phonon interactions.¹⁹ Lead salt semiconductors exhibit the typical positive coefficient of thermal expansion, resulting in a *negative* contribution to the band gap energy dependence on temperature (dE_1/dT). However, unlike several other common semiconductors such as GaAs and Si, the positive contribution to the band gap temperature coefficient of strong electron-phonon scattering,^{18,20–22} on the order of 10^{-4} eV/K , ultimately dominates the overall dE_1/dT behavior for the bulk lead chalcogenides.²⁰

As shown in Figures 1 and 2, this work has found band gap temperature coefficients for OA-capped to range from $13 \mu\text{eV/K}$ ($d = 2.7 \text{ nm}$) to $56 \mu\text{eV/K}$ ($d = 3.5 \text{ nm}$). For EDT-capped thin films, dE_1/dT varies vs. QD diameter as $-112 \mu\text{eV/K}$ ($d = 2.7 \text{ nm}$) to $+17 \mu\text{eV/K}$ ($d = 3.5 \text{ nm}$). Olkhovets *et al.*⁶ measured the exciton transition energy temperature dependence for PbS QDs in glass ranging from 3 nm to 15 nm in diameter. They found that for the smallest sizes, 3 to 4 nm diameter, the slope of dE_1/dT ranges from $-100 \mu\text{eV/K}$ to $50 \mu\text{eV/K}$, in excellent agreement with our measured values for the case of isolated QDs within the OA matrix. Additionally, as seen in Figure 2, replacing the OA with EDT resulted in a reduction of dE_1/dT by $40 \mu\text{eV/K}$ for the 3.5 nm diameter QD film and by $125 \mu\text{eV/K}$ for the 2.7 nm diameter EDT-capped QD film.

Although empirical relationships have been established to model the temperature dependent band gap energy (dE_1/dT) for bulk semiconductors,^{19,23} the mechanisms that may influence the temperature dependence of the effective band gap energy in colloidal QDs are more numerous than simple lattice dilation and electron-phonon coupling. We address these mechanisms of potential temperature dependence here (indicating in square brackets the sign of the contribution to dE_1/dT). (1) [–] Lattice dilation: for PbS QDs, this has been found to be independent of size, and to mimic the behavior of bulk PbS;⁶ (2) [–] quantum confinement effect as a consequence of lattice dilation, estimated to comprise 10%–30%

of observed dE_1/dT depending on PbS QD diameter;⁶ (3) [+], modification of inter-QD spacing induced by thermal expansion of the effective medium (capping ligands and host medium). This effect is expected to be negligible for the isolated OA-capped QDs but may be significant for coupled QDs (vide infra). The reported coefficient of thermal expansion for EDT ($6.25 \times 10^{-4} \text{ K}^{-1}$)²⁴ is approximately one order of magnitude larger than that of PbS and may modify the average inter-QD spacing by as much as $\sim 13\%$ over the temperature range studied. However, the implications of thermal expansion of the film, which may also introduce effects based on stress or strain, are complicated by effects such as the substrate expansion ($\sim 3 \times 10^{-6} \text{ K}^{-1}$ for borosilicate glass) and adhesion, which could result in local variations in the sign of the coupling-induced energy shift of E_1 ; (4) [+ interband and [–] intraband electron-phonon coupling: the interband effect has been estimated by others as $\sim 10^3 \mu\text{eV/K}$,²⁵ and the intraband effect as $-20 \mu\text{eV/K}$ for a 3 nm PbS QD diameter,⁶ and (5) [–] the temperature-dependent effective mass, which in turn influences the confinement energy. Liptay and Ram have estimated²⁵ that this effect accounts for up to $\sim 90\%$ of the difference in dE_1/dT for PbS QDs as compared with bulk PbS, for which $dE_g/dT \approx 320 \mu\text{eV/K}$.²¹

Based on the proposed prominent influence of the effective mass, we consider this factor further within the model of an infinite potential well.²⁵ The confinement energy dependence on temperature is given by $dE_{\text{conf}}/dT = E_{\text{conf}} \times [(-1/m^*) (\partial m^*/\partial T) - (2/R)(\partial R/\partial T)]$. While both terms are expected to be negative, the 2nd term is relatively small based on the coefficient of thermal expansion for PbS of $\sim 2 \times 10^{-5} \text{ K}^{-1}$. Liptay and Ram state a percentage change in effective mass for PbS of $8.5 \times 10^{-4} \text{ K}^{-1}$,²⁵ based on the equations provided by Preier,²⁶ and concluded that the observed temperature dependent PbS QD first exciton peak energy was nearly equal to the bulk PbS band gap dependence modified by the temperature dependence of the confinement energy dE_{conf}/dT . While we have confirmed the positive temperature dependence of the effective mass for bulk PbS,^{26,27} we have not been able to verify either the value ($8.5 \times 10^{-4} \text{ K}^{-1}$) quoted by Liptay and Ram, or any special considerations which may arise in quantum confined structures.

Upon ligand exchange to EDT, increased inter-dot coupling results in a red-shift (Figure 1(b)) via relaxation of the quantum confinement due to increased wavefunction overlap of neighboring QDs, coupled with a distinct reduction in dE_1/dT (Figure 2). The temperature dependent first exciton energy dE_1/dT is now further complicated by the wavefunction overlap between neighboring QDs, since it is a function of inter-QD spacing and the extent to which the wavefunction extends beyond the QD boundary. The increasing inter-QD spacing with temperature due to thermal expansion of the EDT molecules would reduce QD coupling, contributing a blue-shift with increasing temperature, i.e., a positive term to dE_1/dT . Additionally, for $dm^*/dT > 0$, the wavefunction overlap decreases with increasing T because the wavefunction extension is reduced, leading again to a positive contribution to dE_1/dT . The expected result of these contributions would be a larger red-shift at low temperatures and an

increased dE_1/dT for EDT treated films compared with their OA capped counterparts. However, our experimental data for EDT treated films show a *reduction* of dE_1/dT , which is strongest for the smallest QDs, indicating the existence of a stronger negative contribution to dE_1/dT . Szendrei *et al.* investigated PbS QDs of ~ 3.8 nm diameter coupled with 1,2-benzenedithiol (BDT) and found a coupling-induced red-shift of 67 meV (293 K) and 51 meV (5 K).⁷ The deduced value of dE_1/dT is, in both the OA and BDT cases, consistent with the trends we observe for 3.5 nm PbS QD films.

This divergence between the expected influence of inter-QD coupling on dE_1/dT and experimental data requires further consideration. Especially, interesting is the behavior of EDT-treated films which shows that as the QD diameter decreases below 3.1 nm, dE_1/dT decreases and ultimately becomes negative for the 3.1 nm and 2.7 nm diameter coupled arrays. The case of $dE_1/dT < 0$ represents a clear departure from the case of bulk PbS for which $dE_1/dT > 0$. (However, both the nominally isolated PbS QDs as well as the coupled QD arrays show similar behavior with respect to QD diameter. Specifically, dE_1/dT decreases with decreasing QD diameter and the OA-capped sample data project $dE_1/dT < 0$ for $d \approx 2.4$ nm.) A potential effect which merits investigation is the role of capping ligand on effective mass. Veis²⁸ demonstrated that the effective conductivity mass varies with hole concentration in p-type PbS. Milliron²⁹ showed that PbS QD thin films can be made n-type or p-type depending on the selection of the capping ligand, while Brown³⁰ demonstrated that the choice of capping ligand can shift the energy band edges as well as the Fermi level. Should the ligand exchange from OA to EDT result in a reduction of hole concentration, as reported by Klem *et al.*,¹⁴ the contribution of confinement energy (dE_{conf}/dT) to the first exciton temperature dependence dE_1/dT would be expected to increase, resulting in a more negative dE_1/dT due to a reduced effective mass. Another effect which may play a role concerns the influence of temperature on molecular adsorption of the EDT, which has been observed in some systems; a temperature-dependent adsorption would induce a change in the strength of inter-QD coupling.³¹ We identify the behavior in dE_1/dT for coupled QD films as anomalous principally due to the apparent absence of reduced temperature-dependent QD-QD coupling which one would expect based on consideration of thermal expansion (QD-QD spacing) and wavefunction extension.

B. Steady-state photoluminescence

For all QD thin films studied here, as the temperature decreases the PL emission from the PbS QD films is found to increase in intensity, shifts to the red, and exhibits a narrowing of the spectral band width. Figure 3 displays temperature dependent PL for the 2.7 nm QDs measured from 30 K to 295 K. Relative to the OA-capped film samples, the EDT-capped films show red-shifted absorption and emission spectra, and an order of magnitude reduction in the PL peak intensity. Literature reports have shown significant contributions to PbS QD dE_1/dT values from the effects of (a) lattice expansion on confinement energy, (b) temperature-

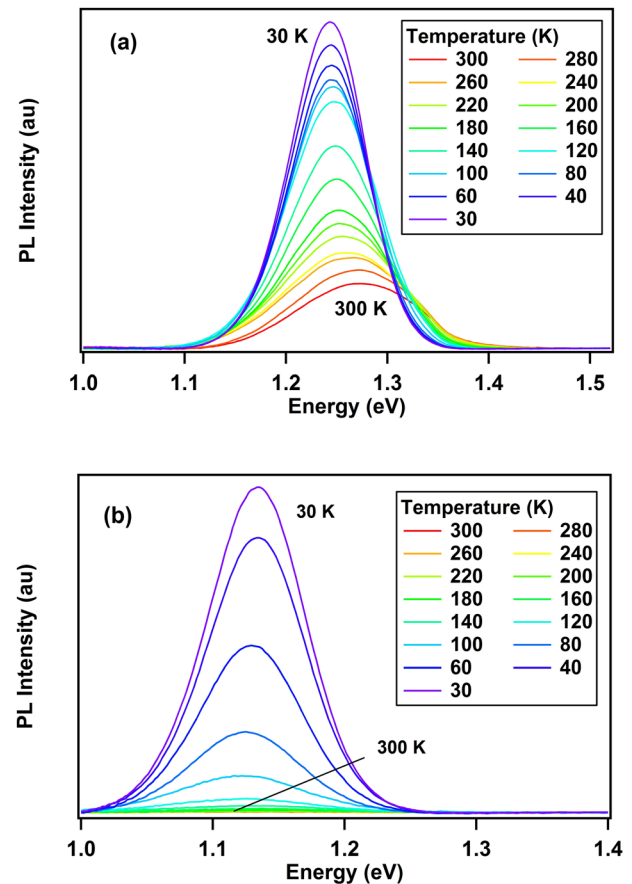


FIG. 3. Temperature dependent PL of 2.7 nm PbS QD films capped with (a) OA and (b) EDT. The EDT film PL is quenched rapidly with increasing temperature. Although the PL peak energy does shift slightly to the red for increased temperature in the range of 30 K to ~ 60 K, the peak energy shifts more strongly to the blue as the temperature increases above 60 K (see Figure 4).

dependent electron-phonon interactions, and (c) the effect on confinement energy of the temperature dependent effective mass. For the case of PbS QD PL, an additional complication arises in that, due to a size- and temperature-dependent non-resonant Stokes shift (*infra vide*), the PL peak energy does not track uniformly with the band gap energy. Nonetheless, numerous studies have settled on fitting PL peak energy vs. T to models derived for the temperature dependence of semiconductor band gap energy.^{4,8,32,33} One such model is that proposed by O'Donnell,¹⁹ which is based on electron-phonon coupling as follows:

$$E_{PL}(T) = E_{PL}(0) + S \langle E_{ph} \rangle \left[\coth \left(\frac{\langle E_{ph} \rangle}{2k_B T} \right) - 1 \right], \quad (1)$$

where $\langle E_{ph} \rangle$ represents the average phonon energy, S is the Huang-Rhys parameter representing the electron-phonon coupling strength, and k_B is the Boltzmann constant. Without detailed analysis, authors applying the O'Donnell relation to the study of PbS QD PL have modified^{4,32} the equation to correlate with the positive temperature dependence observed for lead sulfide (the original sign of the 2nd term is negative). We note here that while fitting PL peak energy vs. T data has resulted in apparently sensible values for the Huang-Rhys parameter and the average phonon energy, the approach is

TABLE I. Temperature dependence of exciton absorption peak and fit results of the modified O'Donnell equation for various QD sizes and capping ligands.

QD diameter (nm)	Capping ligand	dE_L/dT ($\mu\text{eV/K}$)	$E_{PL}(0)$ (eV)	$\langle E_{ph} \rangle$ (meV)	S
2.7	OA	13.5 ± 1.2	1.24 ± 0.006	28.1 ± 3.1	0.89 ± 0.16
	EDT	-110 ± 2.9	1.13 ± 0.002	29.5 ± 2.7	0.98 ± 0.17
3.1	OA	34.5 ± 1.3	1.09 ± 0.005	25.6 ± 1.9	1.54 ± 0.07
	EDT	-45.2 ± 2.9	1.05 ± 0.001	25.3 ± 3.3	1.64 ± 0.13
3.5	OA	56.3 ± 1.6	$0.932 \pm .001$	27.4 ± 1.9	2.67 ± 0.21
	EDT	17.2 ± 1.7	$0.884 \pm .003$	23.9 ± 3.2	2.72 ± 0.12

intrinsically flawed because it does not account for the large QD diameter- and temperature-dependent Stokes shift seen in QDs of PbS and other materials (e.g., CdSe, PbSe, and PbTe).

We include here the results of analyzing our data using this (inappropriate) approach, in order to reveal that this method yields results also in our case. In particular, we fit our PL peak energy vs. temperature data to extract values for $E_{PL}(0)$, $\langle E_{ph} \rangle$, and S; results of the fits are shown in Table I and Figure 4. Extracted values for S range from 0.89 to 2.72, consistently higher than an experimentally measured value of 0.7 via Raman scattering for 3 nm diameter PbS QDs capped with poly(vinyl alcohol).³⁴ Nordin found the average phonon energy to be ~ 24 meV, close to the PbS optical phonon energy of 26.6 meV. For our measurements, the 3.1 nm QD fits yield a similar value, while the 2.7 and 3.5 nm QDs yield $\langle E_{ph} \rangle$ values over a wider range. Nonetheless, as noted above, there exists no sound scientific basis for applying the O'Donnell relation, or any other any other model which is based solely on the modeled temperature dependent band gap energy, to the temperature dependence of the PL peak energy in semiconductor samples exhibiting a large and parameter-dependent PL Stokes shift.

Continuing with an analysis of the PL measurements, our data show an essentially monotonic increase in the PL peak energy with temperature. Gao and Johnson¹⁶ observed a red-shift with increasing temperature for coupled QD films from 13 K to the 80–140 K range, prior to the PL peak shifting to the blue as the temperature increased above 140 K. In our case, a small red-shift is observed in this temperature range only for the smallest QDs in our study. We see that for all QD sizes, and independent of capping ligand, there is a strong temperature dependent Stokes shift which, as described above, deviates from the band gap energy behavior. Our study refers to the nonresonant Stokes shift, which is the difference in photon energy between the peak of the first exciton absorbance and the peak of the PL spectrum. The Stokes shift greatly exceeds the expected shift for splitting of the bright/dark exciton states (on the order of 10 meV).³⁵ Efros *et al.*³⁶ calculated the degenerate dark exciton state to have a Stokes shift up to 100 meV in the case of 1.6 nm diameter CdSe QDs. As noted below, another contribution to the nonresonant Stokes shift observed here for OA-capped QDs is efficient Förster resonant energy transfer (FRET). Litvin *et al.*³³ measured PbS QD PL spectra which fit to the sum of two Gaussian distributions, attributed to the dark exciton state and a mid-gap trap state, and conclude that the exciton state is the primary source of PL emission in PbS

QDs of large diameters ($d > 6$ nm). In contrast, the Stokes shift for smaller dots ($d < 4$ nm) exhibits temperature dependence differing from that of larger PbS QDs; here, the

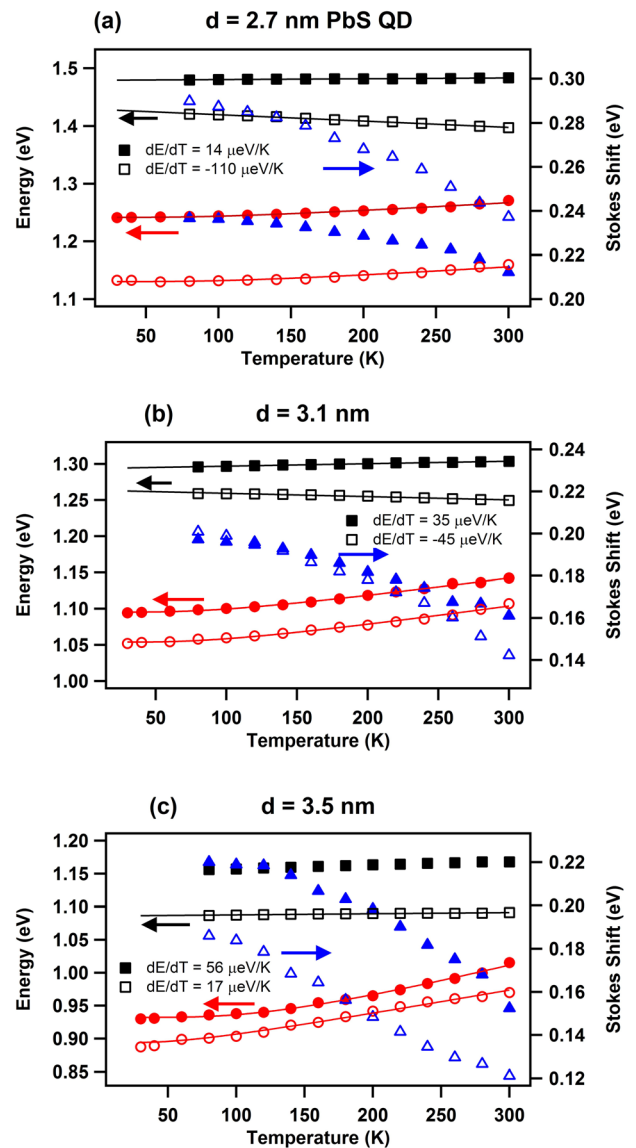


FIG. 4. Temperature dependent absorption (black squares), PL peak energy (red circles), and Stokes shift (blue triangles) for (a) 2.7 nm, (b) 3.1 nm, and (c) 3.5 nm PbS QDs. The solid markers are for OA capped films, while the hollow markers are for EDT capped films. Solid fits are based on linear model for the temperature dependent band gap energy, and on the perfunctory application of the O'Donnell relation for the temperature dependence of the PL peak energy. The large variation observed in the Stokes shift as a function of diameter and temperature highlights the need to model the Stokes shift based on fundamental, measurable parameters.

PL emission has been attributed to a mid-gap state associated with surface traps.³³

Nordin reported a temperature dependent Stokes shift for 4.8 nm diameter PbS QDs,⁴ whose trend matches that observed for our samples, Figure 4 (blue markers). Measuring the PL and absorption spectra at temperatures lower than our system can achieve, Nordin reported that the Stokes shift remained nearly constant from 125 K to 10 K, with a slight reduction upon reaching 3 K. Gaponenko also reported a temperature-dependent Stokes shift.³⁷ Some, but not all, of our films show the onset of a plateau for the Stokes shift in the lower temperature range (Figure 4), possibly indicating that surface passivation plays a role in the temperature dependence of the Stokes shift.

C. Time-resolved photoluminescence

Representative temperature-dependent TRPL measurements are shown in Figure 5 for the 2.7 nm PbS QD films. The OA-capped thin film, comprised nominally isolated QDs which behave similarly to QDs in solution, shows single exponential behavior, whereas the EDT-capped film shows bi-exponential TRPL dynamics. In the case of OA-capped QDs, low temperature decays show a slower rise-time and a longer PL lifetime; the EDT-capped film also shows an increasing PL lifetime with decreasing temperature. The exchange from OA to EDT results in a reduced inter-QD spacing, a change in surface chemistry, and a change in the dielectric constant of effective medium surrounding each QD. With the reduced inter-QD spacing created by ligand exchange to EDT and the resulting increased wavefunction overlap, photogenerated

carriers dissociate readily. The dissociation into free carriers, and the enhanced mobility within the (EDT) film of coupled QDs, allows the photogenerated free carriers to access a larger volume and a larger number of recombination sites within the thin film, resulting in bi-exponential decays.

For all sizes of QDs studied here, the OA-capped films show slowing PL rise time for decreasing temperature, ~ 125 ns rise time for each OA-capped film at 30 K. This behavior has been observed previously in nominally close-packed PbS QD films³⁸ and correlates with FRET which due to increasing confined exciton lifetime becomes increasingly evident at low temperature. Note that in the case of EDT-capped films, the rise time does not noticeably change with temperature. The EDT films exhibit behavior consistent with a dissociation of excitons associated with inter-dot wavefunction overlap, i.e., the excitons dissociate but that the charge carriers then trap at temperatures below about T_Q (vide infra). These data provide additional evidence that the recombination in EDT-capped films occurs from trap states as opposed to originating from excitons.

For isolated QDs at near room temperatures, excitonic recombination processes are predicted to have longer lifetimes for larger diameter quantum dots;³⁹ this behavior has been observed experimentally for PbSe QDs.^{39,40} In contrast, PbS QDs have shown the opposite trend with PL lifetimes increasing for smaller diameter dots;⁴¹ this behavior has been modeled by a three-state process with radiative recombination occurring from a mid-gap state. At low temperatures, the OA-capped QD films of different QD sizes have very similar lifetimes, with no clear trend as a function of QD diameter (Figure 6(a)). All of the EDT treated films show very short lifetimes at high temperatures (Figure 6(b)), while low temperatures show the longest lifetime for the smallest diameter QDs. We apply here a Boltzmann model¹⁶ of thermal quenching to fit integrated PL intensity vs. temperature, for EDT treated films, to identify the temperature associated with thermal quenching

$$I_{PL}(T) = \frac{1}{1 + \exp[(T - T_Q)/\Phi]}, \quad (2)$$

where fitting parameter T_Q is the quenching temperature and Φ indicates the rate of PL quenching as the temperature increases above T_Q —possibly correlating with the energy width of the transport band of states (vide infra). For QD diameters of 3.5 nm, 3.1 nm, and 2.7 nm, temperatures T_Q are 46 K, 51 K, and 66 K, respectively, in good agreement with the findings of Gao and Johnson¹⁶ and correlated with thermal energies of 3.9 meV, 4.4 meV, and 5.7 meV. The spectrally integrated PL intensity vs. temperature data for EDT capped PbS QDs, and the results of the fits, are shown in Figure 7. In contrast, for oleic acid capped QDs, the low temperature PL is plateaued ($T < 50$ K), while increasing temperature results in a slight rise in the integrated PL intensity ($70 \text{ K} < T < 140 \text{ K}$). As the temperature is further increased, the PL intensity slowly decreases due to increased non-radiative recombination within the isolated QDs. As the difference in thermal energy to activate transport-assisted quenching is much lower than the size dependent shift in

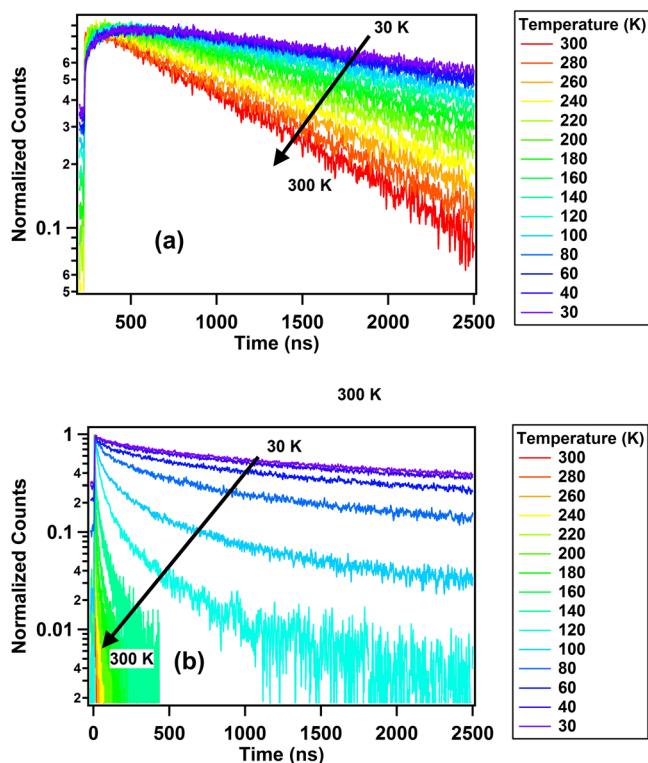


FIG. 5. Normalized TRPL decays for 2.7 nm PbS QD films capped with (a) OA and (b) EDT as a function of temperature. In all cases, TRPL dynamics were measured at the peak of the steady-state PL spectrum.

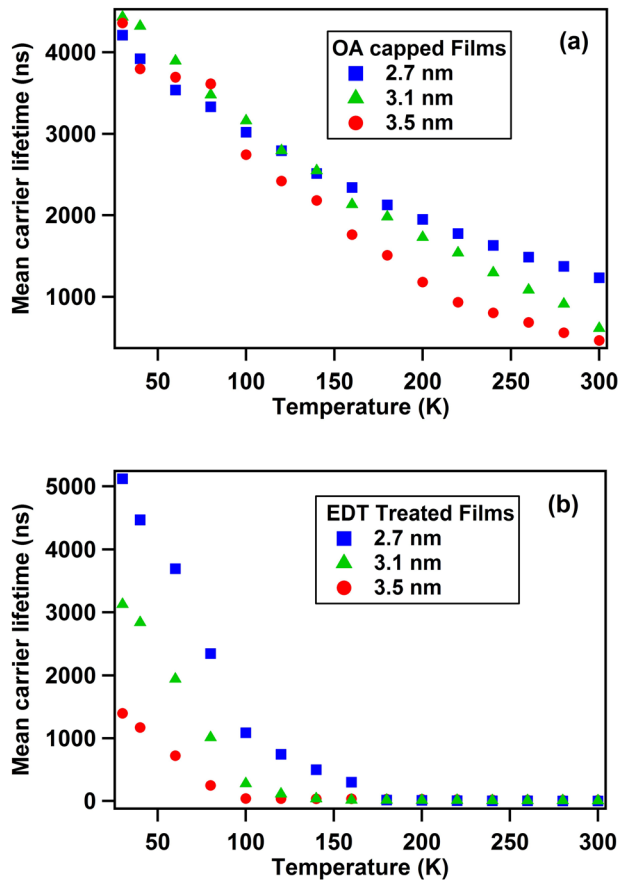


FIG. 6. Mean carrier lifetimes for (a) OA capped films, which exhibit single exponential decay, and (b) EDT capped films, which decay with bi-exponential dependence.

band gap, Gao and Johnson¹⁶ proposed a transport energy level E_T that lies within the density of states (DOS) band tail for treated films. In this model, carriers only require thermal energy sufficient to reach the transport level (less energy than it would take to reach the conduction band) in order to percolate through the QD network and encounter a non-radiative recombination path. Esrev *et al.*⁴² measured an Urbach energy, corresponding to the band edge tail of an

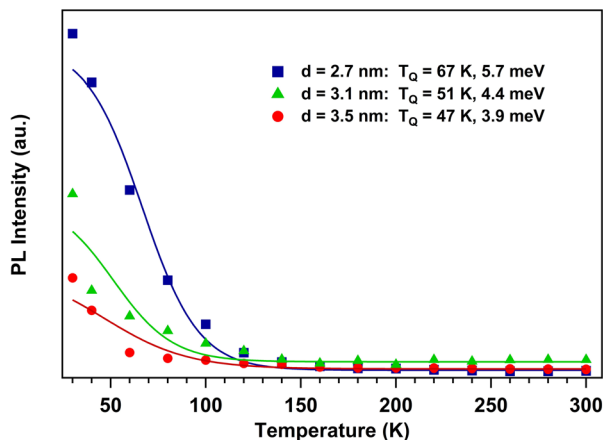


FIG. 7. Integrated PL intensity vs. temperature for each of the three QD diameters. Solid lines show the results of fitting the data to Equation (2), and the legend shows the extracted values for the effective quenching temperature and corresponding thermal energy.

EDT-treated thin film of 1.14 eV PbS QDs, of 14 meV— independent of polydispersity. As smaller QDs have a narrower DOS band tail, the transport level E_T lies higher above the trapped carrier level, requiring more energy to achieve transport and, therefore, PL quenching. Our larger EDT-treated QDs (3.5 nm) experience a faster rate of PL quenching than our small QDs (2.7 nm), in agreement with the size dependent DOS band tail widths depicted by Gao and Johnson.¹⁶ This model agrees with the lifetime trend observed in the EDT-treated QD films, where the lifetimes shorten to tens of picoseconds once the sample meaningfully exceeds that required to excite carriers to the transport level E_T , thereby quenching PL emission.

Nordin measured the temperature dependent TRPL decay of drop cast, OA-capped PbS QD film and found that the data to be bi-exponential (except at 3 K) with lifetimes well over 4 μ s.⁴ The bi-exponential nature of this film could have resulted from poor surface passivation, although this would contradict the longer lifetime. Additionally, Nordin found that the long-lived component became more dominant at temperatures below 100 K. Our OA-capped films were single exponential, and the EDT-capped films showed the fast component as the dominant one over our entire temperature range, with no clear indication of a cross-over at lower temperatures.

IV. CONCLUSION

We have reported on the temperature dependence of the optical absorption, PL spectrum, and PL lifetime for PbS QD films consisting of QDs of varying size and capping ligand. Replacing oleic acid with 1,2-ethanedithiol resulted in a decrease in the first exciton temperature dependence (dE_1/dT), a decrease in the PL intensity, and a reduction in the carrier lifetimes, with a transition from single to bi-exponential behavior. We have highlighted the fact that although several reports have relied on band gap specific models to extract physical parameters from temperature-dependent PL measurements, this approach is fraught with problems arising from extrinsic dependence of the PL peak energy on the Stokes shift—which itself has not been successfully modeled for any general case. At temperatures exceeding ~ 100 to 180 K, the EDT-capped QD films showed complete PL quenching due to thermally activated processes. Thermally activated transport leads to enhanced quenching of PL and reduced mean carrier lifetimes. The temperature dependence of this activation process is size dependent, as evident by the TRPL lifetimes in Figure 6(b), such that efficient transport within the coupled QD films requires more thermal energy for the QDs with larger confinement energy.

Our experimental measurements of the dependence of QD capping ligand (and QD-QD coupling) and diameter on the temperature coefficient of the band gap energy show an unexpected modification when comparing the coupled array of EDT-capped QDs to the nominally isolated OA-capped QDs. Specifically, the values for dE_1/dT are more negative for the coupled QDs which contradicts the behavior expected based on a positive temperature dependence of the effective mass, and on a simple consideration of thermal expansion of

the interstitial EDT molecules within the array. For the two smallest diameter EDT-capped QD samples, we find that dE_1/dT swings negative, in contrast with the well-known positive dE_g/dT values exhibited by bulk PbS, PbSe, and PbTe. A concurring trend exists for the isolated OA-capped QD film: a linear extrapolation of dE_1/dT shows that for QD diameters $d \leq 2.4$ nm, $dE_1/dT < 0$. Thus, a fundamental question exists with regard to the influence of capping ligand, or QD-QD electronic coupling, on the temperature dependence of the first exciton peak energy in PbS QD arrays, and we hope that these data motivate a rigorous theoretical study of the influence of coupling on the temperature dependent first exciton peak energy in QD thin films.

Note that the authors provide access via online supplementary material, to the full raw data for temperature-, coupling-, and diameter-dependent optical transmission, steady-state photoluminescence, and time-resolved photoluminescence.⁴³

ACKNOWLEDGMENTS

The authors gratefully acknowledge funding support from the Air Force Research Laboratory for funding this research under Contract Nos. FA9453-08-C-0172 and FA9453-11-C-0253. In addition, R.J.E. acknowledges support from start-up funds provided by the University of Toledo's Wright Center for Photovoltaics Innovation and Commercialization and the College of Natural Sciences and Mathematics.

¹G.-H. Kim *et al.*, "High-efficiency colloidal quantum dot photovoltaics via robust self-assembled monolayers," *Nano Lett.* **15**, 7691–7696 (2015).
²M. S. Kang, A. Sahu, D. J. Norris, and C. D. Frisbie, "Size- and temperature-dependent charge transport in Pbse nanocrystal thin films," *Nano Lett.* **11**, 3887–3892 (2011).
³J.-H. Choi, A. T. Fafarman, S. J. Oh, D.-K. Ko, D. K. Kim, B. T. Diroll, S. Muramoto, J. G. Gillen, C. B. Murray, and C. R. Kagan, "Bandlike transport in strongly coupled and doped quantum dot solids: A route to high-performance thin-film electronics," *Nano Lett.* **12**, 2631–2638 (2012).
⁴M. N. Nordin, L. Juerong, S. K. Clowes, and R. J. Curry, "Temperature dependent optical properties of Pbs nanocrystals," *Nanotechnology* **23**, 275701 (2012).
⁵J. E. Lewis, S. Wu, and X. J. Jiang, "Unconventional gap state of trapped exciton in lead sulfide quantum dots," *Nanotechnology* **21**, 455402 (2010).
⁶A. Olkhovets, R. C. Hsu, A. Lipovskii, and F. W. Wise, "Size-dependent temperature variation of the energy gap in lead-salt quantum dots," *Phys. Rev. Lett.* **81**, 3539–3542 (1998).
⁷K. Szendrei, M. Speirs, W. Gomulya, D. Jarzab, M. Manca, O. V. Mikhnenko, M. Yarema, B. J. Kooi, W. Heiss, and M. A. Loi, "Exploring the origin of the temperature-dependent behavior of Pbs nanocrystal thin films and solar cells," *Adv. Funct. Mater.* **22**, 1598–1605 (2012).
⁸B. Ullrich, J. S. Wang, and G. J. Brown, "Analysis of thermal band gap variations of Pbs quantum dots by Fourier transform transmission and emission spectroscopy," *Appl. Phys. Lett.* **99**, 081901–3 (2011).
⁹J. Gao, C. L. Perkins, J. M. Luther, M. C. Hanna, H.-Y. Chen, O. E. Semonin, A. J. Nozik, R. J. Ellingson, and M. C. Beard, "N-type transition metal oxide as a hole extraction layer in Pbs quantum dot solar cells," *Nano Lett.* **11**, 3263–3266 (2011).
¹⁰J. M. Luther, M. Law, M. C. Beard, Q. Song, M. O. Reese, R. J. Ellingson, and A. J. Nozik, "Schottky solar cells based on colloidal nanocrystal films," *Nano Lett.* **8**, 3488–3492 (2008).
¹¹M. A. Hines and G. D. Scholes, "Colloidal Pbs nanocrystals with size-tunable near-infrared emission: Observation of post-synthesis self-narrowing of the particle size distribution," *Adv. Mater.* **15**, 1844–1849 (2003).
¹²K. P. Bhandari, P. J. Roland, H. Mahabuduge, N. O. Haugen, C. R. Grice, S. Jeong, T. Dykstra, J. Gao, and R. J. Ellingson, "Thin film solar cells based on the heterojunction of colloidal Pbs quantum dots with Cds," *Sol. Energy Mater. Sol. Cells* **117**, 476–482 (2013).

¹³W. Y. Wu, J. Schulman, T.-Y. Hsu, and U. Efron, "Effect of size nonuniformity on the absorption spectrum of a semiconductor quantum dot system," *Appl. Phys. Lett.* **51**, 710–712 (1987).
¹⁴E. J. D. Klem, H. Shukla, S. Hinds, D. D. MacNeil, L. Levina, and E. H. Sargent, "Impact of dithiol treatment and air annealing on the conductivity, mobility, and hole density in Pbs colloidal quantum dot solids," *Appl. Phys. Lett.* **92**, 212105 (2008).
¹⁵J. J. Choi, J. Luria, B.-R. Hyun, A. C. Bartnik, L. Sun, Y.-F. Lim, J. A. Marohn, F. W. Wise, and T. Hanrath, "Photogenerated exciton dissociation in highly coupled lead salt nanocrystal assemblies," *Nano Lett.* **10**, 1805–1811 (2010).
¹⁶J. Gao and J. C. Johnson, "Charge trapping in bright and dark states of coupled Pbs quantum dot films," *ACS Nano* **6**, 3292–3303 (2012).
¹⁷M. H. Zarghami, Y. Liu, M. Gibbs, E. Gebremichael, C. Webster, and M. Law, "P-type Pbse and Pbs quantum dot solids prepared with short-chain acids and diacids," *ACS Nano* **4**, 2475–2485 (2010).
¹⁸R. Dalven, "A review of the semiconductor properties of Pbte, Pbse, Pbs and Pbo," *Infrared Phys.* **9**, 141–184 (1969).
¹⁹K. P. O'Donnell and X. Chen, "Temperature dependence of semiconductor band gaps," *Appl. Phys. Lett.* **58**, 2924–2926 (1991).
²⁰M. Schlüter, G. Martinez, and M. L. Cohen, "Pressure and temperature dependence of electronic energy levels in Pbse and Pbte," *Phys. Rev. B* **12**, 650–658 (1975).
²¹Z. M. Gibbs, H. Kim, H. Wang, R. L. White, F. Drymiotis, M. Kaviani, and G. Jeffrey Snyder, "Temperature dependent band gap in Pbx (X = S, Se, Te)," *Appl. Phys. Lett.* **103**, 262109 (2013).
²²M. Baleva, T. Georgiev, and G. Lashkarev, "On the temperature dependence of the energy gap in Pbse and Pbte," *J. Phys.: Condens. Matter* **2**, 2935 (1990).
²³Y. P. Varshni, "Temperature dependence of the energy gap in semiconductors," *Physica* **34**, 149–154 (1967).
²⁴E. Zorębski and A. Waligóra, "Densities, excess molar volumes, and isobaric thermal expansibilities for 1,2-ethanediol + 1-butanol, or 1-hexanol, or 1-octanol in the temperature range from (293.15 to 313.15) K," *J. Chem. Eng. Data* **53**, 591–595 (2008).
²⁵T. J. Liptay and R. J. Ram, "Temperature dependence of the exciton transition in semiconductor quantum dots," *Appl. Phys. Lett.* **89**, 223132 (2006).
²⁶H. Preier, "Recent advances in lead-chalcogenide diode lasers," *Appl. Phys.* **20**, 189–206 (1979).
²⁷"Lead sulfide (Pbs) effective masses, conduction band, Fröhlich coupling parameter, Fermi level," in *Non-Tetrahedrally Bonded Elements and Binary Compounds I*, edited by O. Madelung, U. Rössler, and M. Schulz (Springer, Berlin, Heidelberg, 1998), pp. 1–5.
²⁸A. N. Veis, "Energetic spectrum and some properties of lead sulfide implanted with oxygen," *St. Petersburg Polytech. Univ. J.: Phys. Math.* **1**, 1–8 (2015).
²⁹D. J. Milliron, "Quantum dot solar cells: The surface plays a core role," *Nat. Mater.* **13**, 772–773 (2014).
³⁰P. R. Brown, D. Kim, R. R. Lunt, N. Zhao, M. G. Bawendi, J. C. Grossman, and V. Bulović, "Energy level modification in lead sulfide quantum dot thin films through ligand exchange," *ACS Nano* **8**, 5863–5872 (2014).
³¹T. Ju, R. L. Graham, G. Zhai, Y. W. Rodriguez, A. J. Breeze, L. Yang, G. B. Alers, and S. A. Carter, "High efficiency mesoporous titanium oxide Pbs quantum dot solar cells at low temperature," *Appl. Phys. Lett.* **97**, 043106 (2010).
³²M. S. Gaponenko, A. A. Lutich, N. A. Tolstik, A. A. Onushchenko, A. M. Malyarevich, E. P. Petrov, and K. V. Yumashev, "Temperature-dependent photoluminescence of Pbs quantum dots in glass: Evidence of exciton state splitting and carrier trapping," *Phys. Rev. B* **82**, 125320 (2010).
³³A. P. Litvin, P. S. Parfenov, E. V. Ushakova, A. L. Simões Gamboa, A. V. Fedorov, and A. V. Baranov, "Size and temperature dependencies of the low-energy electronic structure of Pbs quantum dots," *J. Phys. Chem. C* **118**, 20721–20726 (2014).
³⁴T. D. Krauss and F. W. Wise, "Raman-scattering study of exciton-phonon coupling in Pbs nanocrystals," *Phys. Rev. B* **55**, 9860–9865 (1997).
³⁵I. Kang and F. W. Wise, "Electronic structure and optical properties of Pbs and Pbse quantum dots," *J. Opt. Soc. Am. B* **14**, 1632–1646 (1997).
³⁶A. L. Efros, M. Rosen, M. Kuno, M. Nirmal, D. J. Norris, and M. Bawendi, "Band-edge exciton in quantum dots of semiconductors with

- degenerate valence band: Dark and bright exciton states," *Phys. Rev. B* **54**, 4843–4856 (1996).
- ³⁷M. S. Gaponenko, N. A. Tolstik, A. A. Lutich, A. A. Onushchenko, and K. V. Yumashev, "Temperature-dependent photoluminescence Stokes shift in Pbs quantum dots," *Physica E* **53**, 63–65 (2013).
- ³⁸S. W. Clark, J. M. Harbold, and F. W. Wise, "Resonant energy transfer in Pbs quantum dots," *J. Phys. Chem. C* **111**, 7302–7305 (2007).
- ³⁹J. M. An, A. Franceschetti, and A. Zunger, "The excitonic exchange splitting and radiative lifetime in Pbse quantum dots," *Nano Lett.* **7**, 2129–2135 (2007).
- ⁴⁰H. Du, C. Chen, R. Krishnan, T. D. Krauss, J. M. Harbold, F. W. Wise, M. G. Thomas, and J. Silcox, "Optical properties of colloidal Pbse nanocrystals," *Nano Lett.* **2**, 1321–1324 (2002).
- ⁴¹E. V. Ushakova, A. P. Litvin, P. S. Parfenov, A. V. Fedorov, M. Artemyev, A. V. Prudnikau, I. D. Rukhlenko, and A. V. Baranov, "Anomalous size-dependent decay of low-energy luminescence from Pbs quantum dots in colloidal solution," *ACS Nano* **6**, 8913–8921 (2012).
- ⁴²P. T. Erslev, H.-Y. Chen, J. Gao, M. C. Beard, A. J. Frank, J. van de Lagemaat, J. C. Johnson, and J. M. Luther, "Sharp exponential band tails in highly disordered lead sulfide quantum dot arrays," *Phys. Rev. B* **86**, 155313 (2012).
- ⁴³See supplementary material at <http://dx.doi.org/10.1063/1.4943066> for the full raw data for temperature-, coupling-, and diameter-dependent optical transmission, steady-state photoluminescence, and time-resolved photoluminescence.